JCTC Journal of Chemical Theory and Computation

Article

pubs.acs.org/JCTC

# Passive Transmembrane Permeation Mechanisms of Monovalent Ions Explored by Molecular Dynamics Simulations

Hui-Yuan Zhang,[†] Qin Xu,[*,†] Yu-Kun Wang,[†] Tang-Zhen Zhao,[†] Dan Hu,[‡] and Dong-Qing Wei[*,†]

[†]State Key Laboratory of Microbial Metabolism and School of Life Science and Biotechnology and [‡]Department of Mathematics, Institute of Natural Science, and MOE-LEC, Shanghai Jiao Tong University, Shanghai 200240, China

Supporting Information

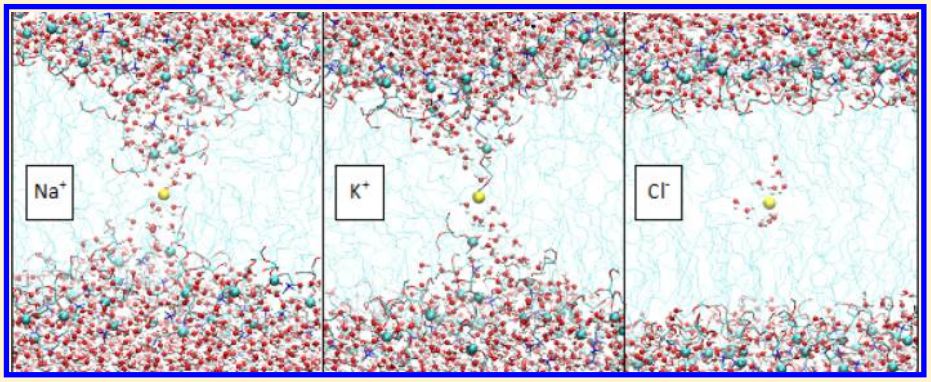


**ABSTRACT:** Passive or unassisted ion permeation through lipid bilayers involves a type of rare events by which cells regulate their salt concentrations and pH. It is important to understand its mechanism in order to develop technologies of, for example, delivering or maintaining small drug-like molecules inside cells. In earlier simulations of passive ion permeations, the commonly used sampling methods usually define the positions of ions relative to the membrane as a measure of permeation, i.e., the collective variable, ignoring the active participations of other particles. Newly defined collective variables involving the movements of ions, lipids, and water molecules allow us to identify the transition paths on the free energy landscape using the 2D umbrella sampling techniques. In this work, this technique was used to study the permeation processes of some well-known ions, sodium, potassium, and chloride. It is found permeations of sodium and potassium are assisted by important lipid bilayer deformations and massive water solvation, while chloride may not. Chloride may have two different possible pathways, in which the energetic favorable one is similar to the solubility-diffusion model. The free energy barriers for the permeation of these ions are in semiquantitative agreement with experiments. Further analyses on the distributions of oxygens and interaction energies suggest the electrostatic interactions between ions and polar headgroups of lipids may greatly influence membrane deformation as well as the water wire and furthermore the free energy barriers of waterwire mediated pathways. For chloride, the nonwaterwire pathway may be energetically favorable.

## 1. INTRODUCTION

Membranes are one of the essential protections for all biological cells mainly by energetic barriers for transmembrane permeations of ions and hydrophilic solutes. At the same time, these barriers may maintain transmembrane ionic gradients, which play important roles in cellular functions like signaling and energy transduction. The impermeability of membrane might be largely ascribed to its main constituents, the lipid molecules. These amphiphilic molecules line up into a bilayer with their headgroups facing the solvents and hydrophobic tails hidden inside the membrane surface and form a relatively impermeable inner layer. However, because of the fluidity of membrane, this inner layer is not so tight and rigid that it prevents any ion permeations.

Decades before, experiments have found ion permeations though a lipid bilayer, for example, $Na^+$, $Cl^-$, $K^+$,[1−5] but the mechanism of ion permeations is still being debated. Two classic mechanisms[6] from experimental literature, solubility-diffusion and pore-mediated permeation, are discussed extensively in particular. Ions are widely believed to pass through lipid bilayers by one or sometimes both of them.[7] In a solubility-diffusion model,[8] permeation is described as a simple process: the molecules dissolve into lipid bilayers, then diffuse through the hydrophobic domain, and dissolve again in bulk at last. This simple mechanism might be true for many hydrophobic molecules; however, the high energy for an ion to expose to the hydrophobic core of the lipid bilayer always challenges it and leads to some models with partial or dynamic solvation of the ion during the permeations. On the other side, in a pore-mediated model[9] a hydrophilic channel is formed throughout the permeation process by deformation of the

Received: July 12, 2016
Published: September 6, 2016





DOI: 10.1021/acs.jctc.6b00695
J. Chem. Theory Comput. 2016, 12, 4959−4969

membrane bilayer into local membrane pores, at least transiently. In this hydrophilic pore, the ions permeate through the membrane plane in an environment of bulk water molecules.

In view of the two mechanisms, Paula and Volkov et al. had tested the dependence of the halide permeability coefficients on bilayers thickness and on ionic size. As a result, it was consistent with permeation of hydrated ions by a solubility-diffusion mechanism rather than through transient membrane pores,[10] while permeation of a monovalent cation such as potassium has been accounted for by a combination of the two mechanisms depending on bilayers thickness.[11]

The pore-mediated mechanism has been approved in simulations recently, for its tolerance of water perturbation and bilayer deformation through the permeating process.[9,12−18] Continuum electrostatics modeling predicted that ions should permeate lipid bilayers in solvation of a bulk of water molecules,[5,19] which were described as water finger, pocket, or funnels in a series of biased molecular dynamics simulations that supported this prediction.[13−17] Wilson and Pohorille conducted MD simulations of unassisted transmembrane transport of $Na^+$ and $Cl^-$.[17] They found successive irregular lipid defects of both sides of bilayers, which lead to the leakage of water and ion molecules, along with the permeation of the ion. Nevertheless, in the simulation of proton permeations, Tepper and Voth observed slight membrane defects and also solvated shells of the proton.[16] Their analysis suggested that transversal water wires would help to stabilize the proton in the apolar bilayer region. An earlier study on the pore-mediated transport of ionic species across a lipid membrane performed molecular simulations on a dipalmitoyl-phosphatidyl-choline bilayer containing a preformed water pore in the presence of sodium and chloride ions and found the transport of the ions through the pores depends strongly on the size of the water channel.[18]

Deformations of lipid bilayers have also been emphasized more in discussions on ion permeation mechanism.[20−23] Tepper and Voth et al.[9] pointed out that current models for passive ion permeation are quite crude and employed multistate empirical valence bond (MS-EVB) and classical molecular dynamics simulations to observe details of ion permeations. They suggested that the permeation mechanism must be a highly concerted one, in which ion, solvent, and membrane coordinates are coupled. Vorobyov and Olson et al.[12] found that membrane perturbations, caused by the movement of an ion, are most critical for explaining the permeation mechanism, which they concluded as an ion-induced defect, leading to both free-energy and diffusion-coefficient profiles that even show little dependence on ion chemistry and charge. Mirjalili and Feig also proposed a new reaction coordinate that allows enhanced sampling of density-driven processes to bias molecular dynamics simulation.[24] They validated the methodology by comparing the theoretical entropy of demixing two ideal gas species and then applied to induce deformation and pore formation in phospholipid membranes within an umbrella sampling framework. An earlier study about permeation of nonaarginine also suggested that the pore-forming paths systematically predicted lower free-energy barriers than the non pore-forming paths.[23]

Even though responses of water and lipids to the permeation of ions have been noticed and discussed, no works have analyzed them quantitatively by far due to lack of proper collective variables in the sampling of a very complicated conformation space to describe the responses of membrane and solvent. In this work, using novel collective variables defined in our earlier work,[25] which are of great help to monitor and control behaviors of both ions and its surrounding molecules, we try to depict a complete picture of the ion permeation process with both ion movement and also responses of solvent and membrane, which may help to reveal proper ways of delivering and maintaining small drug-like molecules inside cells.

## 2. METHODS

**2.1. Redefinition of the Collective Variables for Permeations.** A reasonable way to define the process of ion permeations is by the relative position of ions and the membrane. Traditionally, the membrane was looked at as a stationary plane in most simulations of transmembrane permeations, especially those through ion channels or across-membrane nanotubes. It was easy to transport the solute using a collective variable of the $z$-coordinate of its mass center, which could be also looked at as the relative distance on the $z$-axis between the solute and the horizontal plane with $z$-coordinate as 0, generally the central plane of the membrane. However, the situations in the transmembrane passive ion permeations might be different. Earlier simulations have clearly shown possible local deformation of the membrane surface accompanying the movements of ions into the total membrane plane, so as to keep them out of the hydrophobic interior as possible as they can.[12,16,17,25−27] In these works, biased simulations using the traditional collective variable resulted in an asymmetric concave of the monolayer on the side of ion entry, leading to inconsistency between the central horizontal plane of the total membrane and the midpoint of the upper and bottom hydrophobic−hydrophilic interfaces at the permeation site, which is called the local hydrophobic center here. This midpoint is the actual deepest position for the ion to permeate into the hydrophobic region and possibly the transition state of the permeation. As in the earlier simulations, the hydrophobic center may have a dynamic position related to the local deformations of the bilayer, leading to a dynamic difference between the traditional reference point, the central plane, and the hydrophobic center. Therefore, it might be hard to describe the permeation process using the traditional collective variable. Wang et al. (2014) have noticed the local deformations of bilayers through the charge permeation process and designed a new collective variable to fix the problem; but considering the biology meanings mentioned above, the definition of the collective variable for ion permeation is further developed here as the relative distance between the ion and the local hydrophobic core along the $z$-axis or their relative difference in values of $z$-coordinates

$$\mathrm{CV1} = Z_{\mathrm{ion}} - Z_{\mathrm{lhc}} = Z_{\mathrm{ion}} - \frac{Z_{\mathrm{u}} + Z_{\mathrm{b}}}{2}$$

where the position of the local hydrophobic core along the $z$-axis, $Z_{\mathrm{lhc}}$, is defined as the average of the weighted local heights of the upper and bottom hydrophobic−hydrophilic interfaces, $Z_{\mathrm{u}}$ and $Z_{\mathrm{b}}$, respectively. The calculations on $Z_{\mathrm{u}}$ and $Z_{\mathrm{b}}$ used a successful equation in our earlier simulations[25]

$$Z_{\mathrm{u}} = \sum_i \frac{1 + \cos(\alpha r_{i,\mathrm{u}})}{\sum_j [1 + \cos(\alpha r_{j,\mathrm{u}})]} Z_{i,\mathrm{u}}$$



DOI: 10.1021/acs.jctc.6b00695
J. Chem. Theory Comput. 2016, 12, 4959−4969

$$Z_b = \sum_i \frac{1 + \cos(\alpha r_{i,b})}{\sum_j [1 + \cos(\alpha r_{j,b})]} Z_{i,b}$$

where $\alpha = \pi$ nm$^{-1}$ defines the cylindrical local region with a 1 nm radius in which oxygen atoms of lipid molecules are used to calculate local heights, $i$ and $j$ are indices of the oxygen atoms, u and b denote the upper and bottom interfaces respectively, $Z_i$ are the z-coordinates of oxygen atoms, and $r_i$ is the projected distance of oxygen atoms to the ion in the $x-y$ plane.

Similarly, a second collective variable (CV2) in our earlier simulations is also used here to describe the continuity of water wire (or water bridge, which can be a pure water chain or a mixed polar chain of water molecules and lipid headgroups) in the hydrophobic part of bilayers by combining the distances of the oxygen atoms of adjacent water molecules along the $Z$-axis

$$\mathrm{CV2} = \left[ \sum_i (Z^s_{i,O} - Z^s_{i+1,O})^\beta \right]^{1/\beta}$$

where $\beta = 6$ and $Z^s_{i,O}$ are the $z$-coordinates of the oxygen atoms with the index $i$ in sorted order. The strong power of $\beta = 6$ here makes the CV2 very sensitive to the breaking of the water wire. Large distances of the broken part of the water wire would contribute to CV2 mostly and increase CV2 importantly.

**2.2. Searching for Minimum Free Energy Transition Pathways.** The earlier simulations on the permeation of a single-charged methyl guanidine resulted in a simple symmetric minimum free energy transition path along the CV1, with the transition state located in the midpoint of the permeation pathway. Therefore, the key part to identify its minimum free energy transition pathways is to find its transition state configuration, and therefore the ion will just run along its minimum free energy transition path when it is released from the transition state.[25] This is consistent with the symmetric property of the model membrane. Considering the similarity between single-positively charged ions and methyl guanidine, and also a number of simulation works have shown that the highest energy barrier of the permeation process is in the center of lipid bilayers,[9,12,25,28,29] it is reasonable to presume the transition state should be in the center of the $z$-axis variable (i.e., CV1). So, transition state configuration must be one of the configurations when a single ion is fixed in the center of bilayers. Nevertheless, since we are looking for a transition state in the minimum free energy transition path, it has to be a point with minimum energy barrier along the water wire axis. According to the Boltzmann equation,[30] if a configuration has lower free energy, it will appear more frequently, so among all configurations the dominant ones should have the lowest free energy. Therefore, when releasing ions from the transition-state positions, they would more likely follow a pathway closely around the minimum free energy paths.

To find the transition-state configurations, we fixed each single ion in the hydrophobic core for 120 ns and picked up the conformations that appear the most times as the ensemble of its transition state configuration. All the configurations are differentiated by continuity of the water wire (i.e., CV2). Twenty representative snapshots were randomly picked out of the ensemble as initial configurations to start permeations, from which ions are released for 20 times each. According to the changes in CV1 and CV2, most of the trajectories are consistently along a tube around the minimum free energy path, although with some fluctuations, or moving to either side of the membrane. Therefore, after mirroring the CV1 to the same side of the membrane, the minimum free energy paths for the permeations were depicted as the average of the distributions in CV1 and CV2 (Figure S1). Since two populated configurations were found for $Cl^-$, two ensembles were constructed for releasing, and two different paths were depicted.

**2.3. MD Simulations and Determinations of Free Energy Changes.** A solvated membrane of 126 palmitoyloleoylphosphatidylcholine (POPC) lipids was simulated in a box of $6.41 \times 6.41 \times 7.63$ nm$^3$, with the membrane perpendicular to the $z$-axis. Also, 21 pairs of $Na^+$ and $Cl^-$ ions were placed in the system, together with 4905 water molecules. The lipids were modeled with the force field by Ulmschneider et al.,[31] and the OPLS-AA TIP3P model and ions model were used for water molecules and ions, respectively. MD simulations were performed in the $NP_n\gamma T$ ensemble on Gromacs, at normal pressure ($P_n$ = 1 atm), with a Nose-Hoover thermostat ($T$ = 310 K, $\tau_T$ = 0.5 ps). The time step is 2 fentosecond (fs), and a typical simulation lasts about 1400 ns (ns). The nonbonded interactions were computed using the particle mesh Ewald method.[32,33]

Along a proposed pathway, umbrella sampling was performed by harmonic potentials on the two collective variables, CV1 and CV2. The permeations from the hydrophobic core to the equilibrated state out of the membrane were completed by about 30 windows (27 windows for $Na^+$, 29 windows for $K^+$, 33 and 30 windows for $Cl^-$ along the two pathways), and each window was simulated for 50 ns including 10 ns equilibrium. All the conformational distributions in these simulations were integrated into overall free energy profiles with the biasing potentials adjusted by the weighted histogram analysis method (WHAM).[34] Especially, a 2D WHAM software was used here.[35]

## 3. RESULTS AND DISCUSSION

**3.1. The Transition States.** As discussed in the Methods, the transition states for passive ion permeations through the membrane should be at the local hydrophobic core at the permeations site. Therefore, with the ions restrained around the local bilayer center by CV1, we ran 120 ns simulations to explore the more stable configurations near the real transition states.

Representative configurations of the transition state conformation ensembles are shown in Figure 1 on the right side for each ion. It seems that all the ions are some kind of water solvation shell. Also, the number of water molecules around these ions within the first hydration shell (Figure 4D) when the ion in the center is generally the same as when it is outside the bilayer suggests all the ions are necessarily hydrated even in the hydrophobic core.

In the transition state configurations of $Na^+$ and $K^+$, both of the two monolayers concave deeply into the membrane plane, resulting in a very thin hydrophobic layer penetrated by a cluster of water, which is bridged by the ion. The hydrogen bond network between the ion, the water molecules, and the polar headgroups of lipids seems like an incomplete water pore through the membrane. Some early works have noticed this kind of big deformation caused by some cations and attribute it to the internal dipole potential of lipid molecules in the bilayer, which is proposed to have the positive end inside and the negative end outside.[36,37] Interestingly, when looking into local membrane deformation, Vorobyov et al. found hydrocarbon


DOI: 10.1021/acs.jctc.6b00695
J. Chem. Theory Comput. 2016, 12, 4959−4969

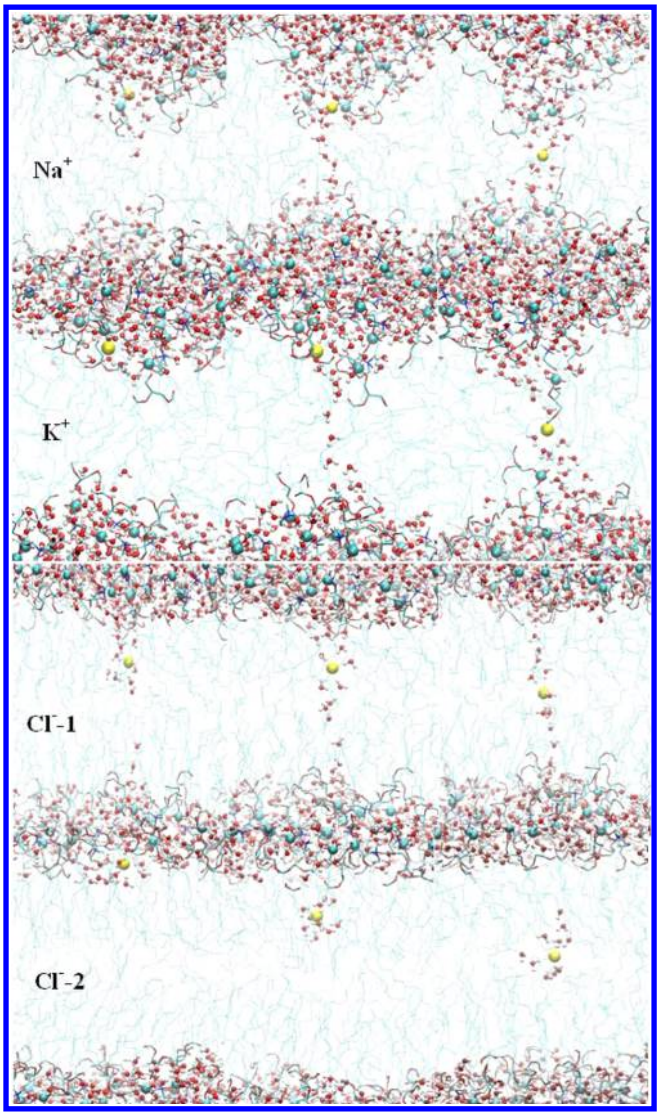


**Figure 1.** Snapshots of ions $Na^+$, $K^+$, and $Cl^-$ when released from the membrane center (right panels). The water-wire path and the nonwaterwire path for $Cl^-$ permeations are indicated by $Cl^-$-1 and $Cl^-$-2, respectively. For clarity, the polar headgroups are represented by thick colored sticks and the phosphorate by blue balls, and the carbon tails are shown by cyan thin sticks; the water molecules are represented by balls and sticks, and the ions are represented by space filling in yellow.

electronic polarizability causes dramatic changes in ion solvation free energy, as well as a significant change (~0.4 V) in the membrane dipole potential, and little change in membrane permeation energetics occurs.[38] They attributed this to compensation of solvation terms from polar and polarizable nonpolar components within the membrane; but in our transition state configurations, it seems electrostatic attraction between the positive charged ions and the partial negative charged headgroups at least contributes partially to the membrane deformation, since the molecules are in a uniform direction that has the polar oxygen atoms pointing toward the ion.

On the other hand, the transition state configurations of $Cl^-$ are quite different. Although two possible configurations were found for $Cl^-$, neither of them has important membrane deformations. In the first transition state configuration, together with the ion, a single-file water chain links through the upper and bottom hydrophobic−hydrophilic interfaces of the two monolayers. The second transition state configuration of $Cl^-$ is more compatible with the solubility-diffusion model, where the ion is surrounded by a shell of water molecules that is isolated from either hydrophobic−hydrophilic interface. The two configurations were transformed to each other several times in the 120 ns MD simulations, and, once formed, either can stay stable as long as several nanoseconds. This result may suggest two metastable states of $Cl^-$ in the center of the lipid bilayer with relatively low energetic barriers. In the case of $Cl^-$, no important deformations of bilayers were found.

**3.2. The Permeation Pathways.** As described in the Methods, the most possible permeation pathways of the ions $Na^+$, $K^+$, and $Cl^-$ are elucidated by average of repeated permeations from the local center of the bilayer. Snapshots of the permeations are shown in Figure 1. Several interesting parameters from these umbrella sampling windows were summarized in Figures 2, 3 and 4, so as to compare the different permeation pathways of these ions.

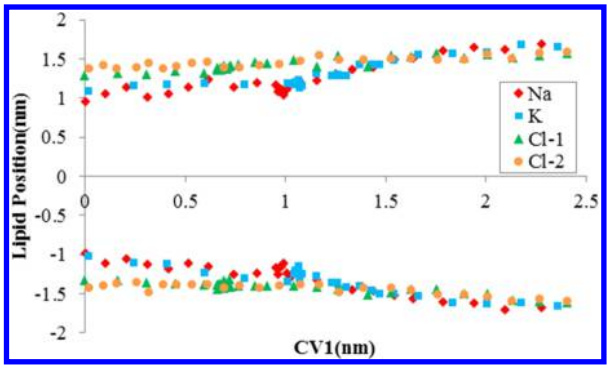


**Figure 2.** Average positions of lipid headgroups along the *z*-axis when $Na^+$ (red dimond), $K^+$ (cyan square), and $Cl^-$ (green triangle along first path and orange round dot along second path) permeate from the interior out of the membrane, where the positions of ions are defined by CV1.

The permeation pathways of $Na^+$ and $K^+$ are quite similar. In the transition states, the hydrophobic−hydrophilic interfaces of both monolayers concave into the hydrophobic core, with clusters of water molecules and lipid headgroups from both monolayers filling the concaved membrane surfaces and being

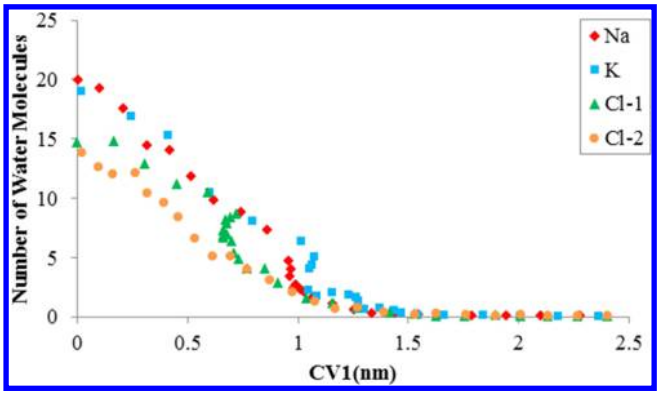


**Figure 3.** Average number of water molecules merged into the hydrophobic core of the membrane bilayer (between −0.7 and 0.7 nm).



DOI: 10.1021/acs.jctc.6b00695
J. Chem. Theory Comput. 2016, 12, 4959−4969

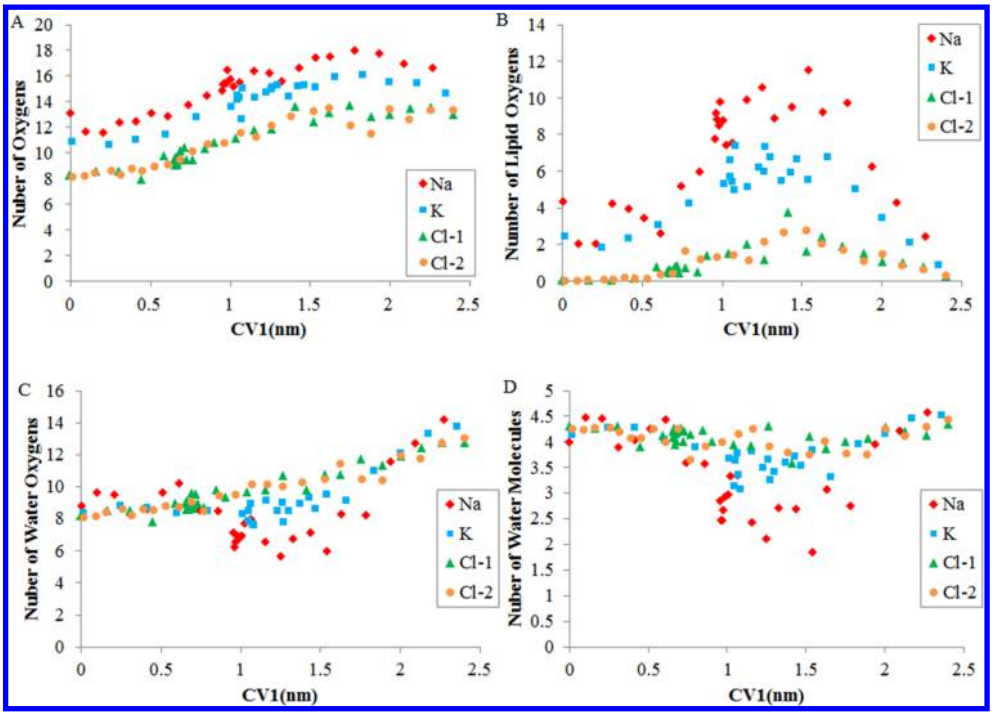


**Figure 4.** (A) The number of polar oxygen including (B) lipid oxygen and (C) water oxygen within 0.5 nm of the ion during the permeations. (D) The number of water oxygens around ions within the first hydration shell, with the radius as 0.27 nm for $Na^+$, 0.3 nm for $K^+$, and 0.34 nm for $Cl^-$ from ref 40. The symbols for the ions are the same as in Figure 2.

bridged by the ion. Although greatly deformed, the thick POPC membrane is not fully penetrated by a complete membrane pore but by a short water wire together with the ion in the hydrophobic core. From another view, the two monolayers are attracted to the ion so close that its solvation shell could easily fuse with water molecules from the hydrophobic−hydrophilic interfaces to link through the solvents on both sides. When the ion is moving outward, the deformations of the two monolayers are both reduced, with the ion closely interacting with polar oxygens of water molecules and lipid headgroups. At the same time, the water bridge between them is extended into a thin water wire and soon broken.

As shown in Figure 2, the deformations of the membrane are obviously different between the permeations of the positively charged ions and the negatively charged $Cl^-$. In $Na^+$ and $K^+$ permeations, the average positions of the polar lipid headgroups vary with the positions of the ions. When CV1 is decreasing less than 2 nm, the ions enter the membrane plane, leading to the average positions of the lipid headgroups to decrease slowly at the same time, which can be as low as less than 1 nm when the ion is in the hydrophobic center. This change means a local concave of the monolayer surface to help shorten the water wire.

The permeation pathways of $Na^+$ and $K^+$ are quite similar to our early simulations on methyl guanidine,[25] which has a positive charge too. Therefore, a similar permeation mechanism might be suggested for monovalent cations in POPC bilayers. A positively charged ion or residue is easy to permeate to the hydrophobic−hydrophilic interface, where the partially negative charged polar oxygens and also the hydrophobic core that consists of carbon chains stop it from further permeation. Here, probably due to thermal dynamic motions, or partially assisted by electrostatic attractions as suggested in a recent model,[39] both of the monolayers locally deform to each other until a water wire links the two interfaces, which makes it easier for the ion to solvate through the hydrophobic core into the concave of the monolayer on the other side. When the ion further moves out of the hydrophobic core, both monolayers deform back keeping the ion mainly at the hydrophobic−hydrophilic interface and following that the water wire is broken soon. Finally the ion is released into the solvent on the other side of the membrane. Because no complete water pore is formed in this permeation pathway, it is called Water-Wire Mediated Mechanism. Comparing with our earlier results from simulations on methyl guanidine, here we particularly notice the possible roles of the electrostatic interactions between the ion and polar lipid headgroups, which helps to shorten and stabilize the water bridge. The reason for this hypothesis is mainly because of the different pathways of $Cl^-$ permeations discussed below.

As shown in the lower figures of Figure 1, the permeation paths of $Cl^-$ are quite different. When $Cl^-$ enters the hydrophobic−hydrophilic interface, no important deformation of the lipid bilayers arises. Also in Figure 2, in the case of $Cl^-$ permeations, there are no significant changes in the average positions of the lipid headgroups when the CV1 value is low, suggesting no important deformation of the monolayers accompanying the entrance of $Cl^-$. In the whole changing range of CV1, the average positions of lipid headgroups mostly stay stable.

When $Cl^-$ permeates further through the hydrophobic environment, the high dehydration energy forces it to keep some solvation shell with it. However, two ways of the solvation were observed in our simulations, which may suggest two possible paths for $Cl^-$ permeations hinting different mechanisms. The first path $Cl^-$-1 is still like a water-wire mediated mechanism. When $Cl^-$ permeates into the hydrophobic domain, a single-file water wire linking it to the two interfaces is formed dynamically and transiently, somewhat shielding $Cl^-$ from hydrophobic interactions with the lipid tails. Comparing


DOI: 10.1021/acs.jctc.6b00695
J. Chem. Theory Comput. 2016, 12, 4959−4969

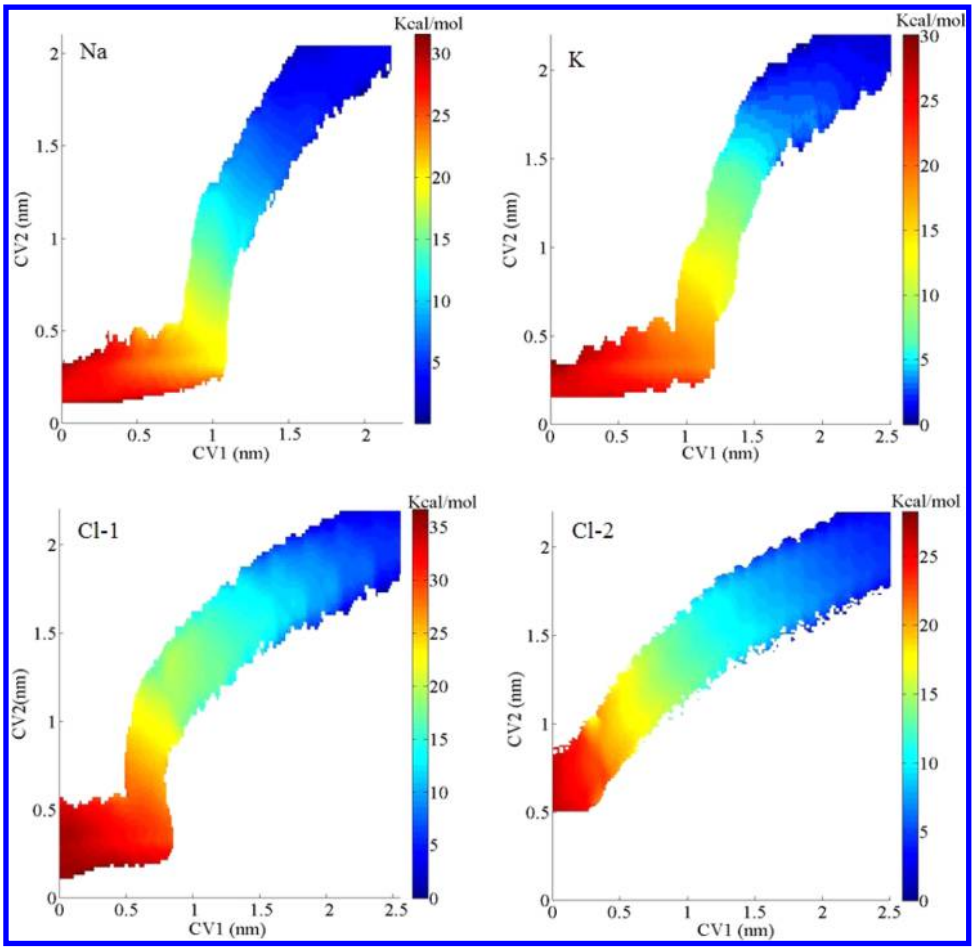


**Figure 5.** Free energy changes along the permeations of ions $Na^+$, $K^+$, and $Cl^-$. The two possible pathways for $Cl^-$ permeations are indicated by Cl-1 and Cl-2.

with the one in $Na^+$ and $K^+$ permeations, this water bridge is longer and less stable. Oppositely, the other path $Cl^-$-2 is more like a solubility-diffusion mechanism. Without a transmembrane water bridge formed, the ion enters into the hydrophobic core with a cluster of water molecules as its solvation shell. Then this group of ion−water cluster diffuses through the hydrophobic core and arrives to the other side and finally merges into the solvents on the other side.

In Figure 3, the solvation of ions during permeations was analyzed by counting the number of water molecules into the membrane plane. To avoid the influences of lipid headgroups which may dive deep in the process, we strictly define the counting range as −0.7 nm < CV1 < 0.7 nm. From the figure, it is obvious that $Na^+$ and $K^+$ permeations have more water molecules entering the central layer of the membrane. Corresponding to the snapshots, the possible reason is the stronger water bridge. The sharp rise of the numbers at CV1 = 1 nm may suggest the key point to form the water bridge. Similarly, the formation of a water bridge is also suggested by the sudden rise of water numbers at CV1 = 0.7−0.8 nm for the $Cl^-$-1 path, although the water molecules solving the $Cl^-$ ion are relatively less. However, in the range between 0.3 and 0.7 nm, the number of water molecules in the $Cl^-$-1 path is comparable to those for $Na^+$ and $K^+$, where all these ions just enter the membrane hydrophobic core and the water bridge may be all thin in the central region. At last, the number of water molecules in the $Cl^-$-2 path increases steadily to about 13 when CV1 is less than 0.2 nm, where the solvation shell stays stable when $Cl^-$ diffuses in the deep hydrophobic core.

To decompose the actual interactions with the ions during their permeations, in Figure 4 the polar oxygens surrounding the ions are counted (Figure 4A), including those from lipid headgroups (Figure 4B) and from water molecules (Figure 4C). Within 0.5 nm, the total number of polar oxygens around $Na^+$ and $K^+$ is always 3−5 higher than those around $Cl^-$ in either path. More careful counting found that the number of water oxygens around these three ions is actually the same, and the only difference is more lipid oxygens interacting with the positive ions, consistent with our hypothesis on the electrostatic interactions between ions and lipids. Comparing with $K^+$, $Na^+$ has 1−2 more oxygens around, which may be explained by its smaller hydration shell of 0.27 nm than the 0.3 nm of $K^+$,[40] leading to more oxygen in the second hydration shell counted. However, at the hydrophobic−hydrophilic interface with CV1 between 1 and 2 nm, $Na^+$ and $K^+$ interact with less water molecules than $Cl^-$ but with much more lipid oxygen, suggesting more lipid oxygens compete with water by the strong electrostatic attraction. On the other hand, in either path of $Cl^-$ permeations, this change of hydration is not observed. The minor increase in lipid oxygens at the interface with CV1 around 1.5 nm may only come from steric approaching.

### 3.3. The Free Energy Changes of Ion Permeations.

Two-dimensional free energy change profiles were calculated by WHAM to describe the paths of ion permeations. As shown


DOI: 10.1021/acs.jctc.6b00695
J. Chem. Theory Comput. 2016, 12, 4959−4969

in Figure 5, the free energy barrier of $Na^+$ and $K^+$ permeation is about 26.2 and 26.6 kcal/mol, respectively. The free energy for $Cl^-$ to permeate through the first transition path is about 26.9 kcal/mol and is about 20.5 kcal/mol via the second path. Also, permeability coefficients of ions have been roughly estimated by a formula proposed by our earlier work.[25] It is noteworthy that the errors estimated for $Na^+$, $K^+$, $Cl^-$-1, and $Cl^-$-2 are quite large, respectively 113%, 55%, 83%, and 50%. Compared with some earlier experiment results (Table 1), the free energy barrier of $Na^+$, $K^+$, and $Cl^-$-2 from our work is consistent with the work from D. Papahadjopoulos (see footnote a in Table 1), particularly for $Cl^-$-2, considering their estimated errors. As for the permeability coefficients, $Cl^-$-2, which has the smallest estimated error, is at the same magnitude of most works except for the work of S. Paula et al. (see footnote b in Table 1); but interestingly, the difference in orders of the magnitudes between $K^+$ and $Cl^-$-2 in their work (see footnote b in Table 1) is almost the same with ours. $Na^+$ and $K^+$ in our work is 1−3 orders of magnitude smaller than the works of the other three (see footnotes a and c Table 1); but considering the large errors in our estimation and also among the three (see footnotes a and c Table 1), it may be suggested that large errors of permeability coefficients may exist extensively. Generally, free energy barriers from our simulations are in semiquantitative agreement with experiments. Since we are aimed at looking for the ion permeation mechanisms, and for the responses of surrounding molecules to the permeation of ions, it is reasonable to conclude the permeation pathways found in our simulations are quite close to the real minimum free energy path, which means the mechanisms we found probably work in reality.

**Table 1. Ion Permeability Coefficients in Different Bilayers**

| bilayer | ion | $P^e$($10^{-12}$ cm/s) | Wpeak[e](kcal/mol) |
|---|---|---|---|
| bovine brain PS[a] | $Na^+$ | 0.16 | 23.5 ± 2.7 |
| | $K^+$ | 0.91 | 22.5 ± 3.9 |
| | $Cl^-$ | 6.5 | 20.8 ± 0.4 |
| DOPC[b] | $K^+$ | 3.47 | |
| | $Cl^-$ | 12100 ± 1400 | |
| egg lecithin[c] | $Na^+$ | 0.021−0.029 | |
| | $Cl^-$ | 55 | |
| ox-brain PS[c] | $Na^+$ | 0.055 | |
| | $Cl^-$ | 15 | |
| POPC[d] | $Na^+$ | 0.0008 ± 0.0009 | 26.2 |
| | $K^+$ | 0.0033 ± 0.0018 | 26.6 |
| | $Cl^-$-1 | 0.0006 ± 0.0005 | 26.9 |
| | $Cl^-$-2 | 16.36 ± 8.2 | 20.5 |

[a]Experimental results from Papahadjopoulos et al.[41] at 309 K, and peak values are estimated at 300 K. [b]Experimental results from Paula et al.[10,11] at 303 K. [c]Experimental results from Hauser et al.[5] at 303 K. [d]Our work simulated at 310 K. [e]P for permeabilities; Wpeak for free energy barriers.

In regard to waterwire mediated transition pathways, i.e. $Na^+$, $K^+$, $Cl^-$-1, at the position where water molecules begin to aggregate to form a water wire (Figure 3, CV1 ≈ 1 nm for $Na^+$ and $K^+$, CV1 ≈ 0.7−0.8 nm for $Cl^-$-1), there is a significant rise in energy fluctuations caused by CV2, as shown in Figure 6. On the other hand, energy fluctuations in $Cl^-$-2 are rather stable along CV1. No doubt that CV2, the collective variable for measurement of water wire, has great influence on the calculation of free energies. When putting the three waterwire mediated pathways together, it is easy to find the water wire constructed with more water molecules, which is thicker, will be likely to stay well connected (i.e., CV2 is smaller) for a longer distance in CV1; more surprisingly and importantly, the pathway in which a thicker water wire is formed is likely to have a lower free energy barrier. In addition to water wires, membrane deformations, which are related to strong or weak electrostatic interactions between the ion and lipids, may also have great influence on the free energy barriers. To look into the interactions between the ion and surrounding molecules, we calculated the short-range Coulomb force and Lennard-Jones potential between the ion and lipids, between the ion and water solutions, and also between the ion and the system (the interaction energy is referred to as the sum of the Coulomb force and Lennard-Jones potential), as shown in Figure 7. To investigate the role of the Coulomb force, we also drew it along the interaction energy (Figure 7A and 7B) and found the interaction energy was largely dependent on the Coulomb force, or electrostatic energy, and the changing trend is exactly the same with it. Among the four pathways, the general trend of sodium and potassium in interaction energies with lipids and water solution is quite similar. Not surprisingly, the interaction energies between the two pathways of chloride are almost the same, of which the trend is totally different with the cations. In consideration of the similar transition states, pathways as well as the interaction energy trends between sodium and potassium, it is fair to suppose that there probably exists a uniform permeation mechanism, i.e. a waterwire mediated mechanism, for cations in thicker lipid bilayers, like POPC, whereas it is totally different in the situation of anions.

When the sodium or potassium ion stays in bulk, as shown in Figure 7A, there are almost no interactions between the ion and the far-away lipids. Compared with potassium, sodium interaction energy with water solution is about 25 kcal/mol lower, and chloride is about 15 kcal/mol lower (Figure 7B). It seems that sodium is the most favorable ion for water solution, next is the chloride, and last is the potassium. After checking the experiments about ion solvation energies in water,[29,42−46] no explicit results about the three ions were found. However, the comparison between $Na^+$ and $Cl^-$ was found, that the solvation energy of $Na^+$ is about 24 kcal/mol lower than $Cl^-$.[46] Also, $K^+$ is about 17 kcal/mol higher than $Na^+$.[42] Considering the experimental energy values reported may not be accurate since these were determined under different extrathermodynamic assumptions by different groups,[45] it is not proper to just compare these results directly. When sodium or potassium gets close to lipid bilayers, CV1 from 2.5 to 2 nm, the interaction energy with lipids starts to fall rapidly, and when sodium or potassium gets into the hydrophilic layer of lipids, CV1 ≈ 2 nm, the interaction energy with lipids falls faster. In general, the interactions with lipids appear to be most favorable when the sodium or potassium is around the hydrophilic headgroups of lipids, i.e. CV1 = 1−2 nm. In the force field of POPC molecules, although the lipid molecule is neutral as a whole, all the atoms with a charge over 0.5e are negatively charged except for a phosphorus atom which is surrounded by four negative oxygen atoms. Since the phosphorus atom hardly has a chance to interact with other atoms closely, it seems the negative charges are more concentrated, and therefore this advantage of negative charges made lipid headgroups prefer to interact with cations. It is noteworthy that the force field used here is obtained from experiments. When the ion stays in the hydrophilic domain of lipids, CV1 = 1−2 nm, there are huge


DOI: 10.1021/acs.jctc.6b00695
J. Chem. Theory Comput. 2016, 12, 4959−4969

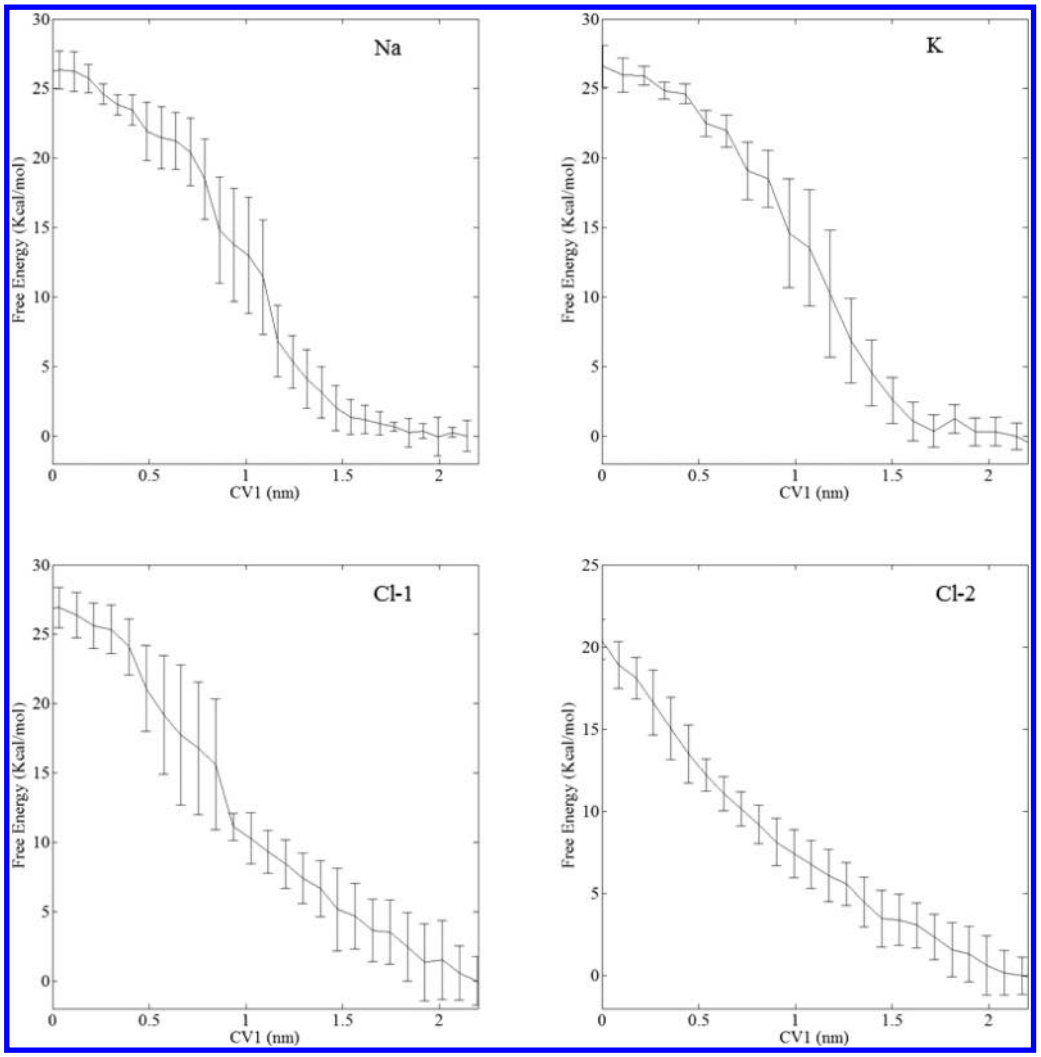


**Figure 6.** Projection of the potential of mean force of ion permeations along CV1 with statistical error indicated.

fluctuations in the interaction energy of $Na^+$ or $K^+$ with lipids. Also, every local minimum of interaction energy of $Na^+$ and $K^+$ (Figure 7A) is exactly corresponding to a local maximum number of lipid oxygen atoms around (Figure 4B), which suggests it is the many more interactions of $Na^+$ of $K^+$ with lipid oxygen atoms that make the interaction energy with lipids reach its local minimum. Furthermore, lipid oxygen atoms are the key part of interactions between lipids and $Na^+$ or $K^+$, or even cations, for which the lipid hydrophilic region where oxygen atoms are greatly abundant becomes a comfort zone for $Na^+$ and $K^+$. Especially, the interaction of $Na^+$ with lipids is much stronger than $K^+$, which agrees well with the inference above that it is the smaller ionic size of $Na^+$ that makes $Na^+$ have stronger interactions or attractions with lipid oxygen. When CV1 ≈ 1−1.1 nm, $Na^+$ or $K^+$ has reached the hydrophilic−hydrophobic interface, a strongly positive carbon atom along with 4 negative oxygen atoms makes the interaction energies between lipids and the ion go through comparatively large fluctuations. Then, when CV1 < 1 nm, the ion begins to permeate through the hydrophobic domain of lipid bilayers, and the interactions between $K^+$ or $Na^+$ and lipids start to weaken too. The local minimum of $K^+$ appears at CV1 = 1.1 nm suggesting the exact location of the 4 oxygen atoms of lipid on the hydrophilic−hydrophobic interface, whereas the local minimum of $Na^+$ appears at CV1 = 1 nm. It is easy to suppose $Na^+$ has begun to pull or attract the lipid headgroups down toward the hydrophobic center, so that the local minimum position drops to 1 nm. After that the ion permeates through the hydrophobic core, when CV1 decreases from 1 to 0 nm. Since the ion goes far from the polar headgroups, the interaction energy increases then. Generally, even with much larger fluctuations, interaction energy between $Na^+$ and lipids is still lower than that between $K^+$ and lipids, and the differences may come from the more pronounced membrane deformations caused by $Na^+$, by which lipid oxygen atoms are much more in its surroundings.

To understand the whole process of ion permeation, interaction energies between water solution and the ion are also calculated in Figure 7B. When the $Na^+$ or $K^+$ is around the lipid headgroups, CV1 = 1−2 nm, the interactions between water and the ion become weaker, and the interaction energy increases about 14 kcal/mol (Figure 7B), probably caused by the decrease of water molecule amount. Also the number of water molecules around $Na^+$ is less than that of $K^+$, but there is no significant difference in their interaction energies except larger fluctuations in $Na^+$. Entrance of the ion and water molecules decreases the hydrophobicity in membrane core, and a water wire is then formed. Compared to $K^+$, $Na^+$ has about 20 kcal/mol lower interaction energy with water; a thicker and


DOI: 10.1021/acs.jctc.6b00695
J. Chem. Theory Comput. 2016, 12, 4959−4969

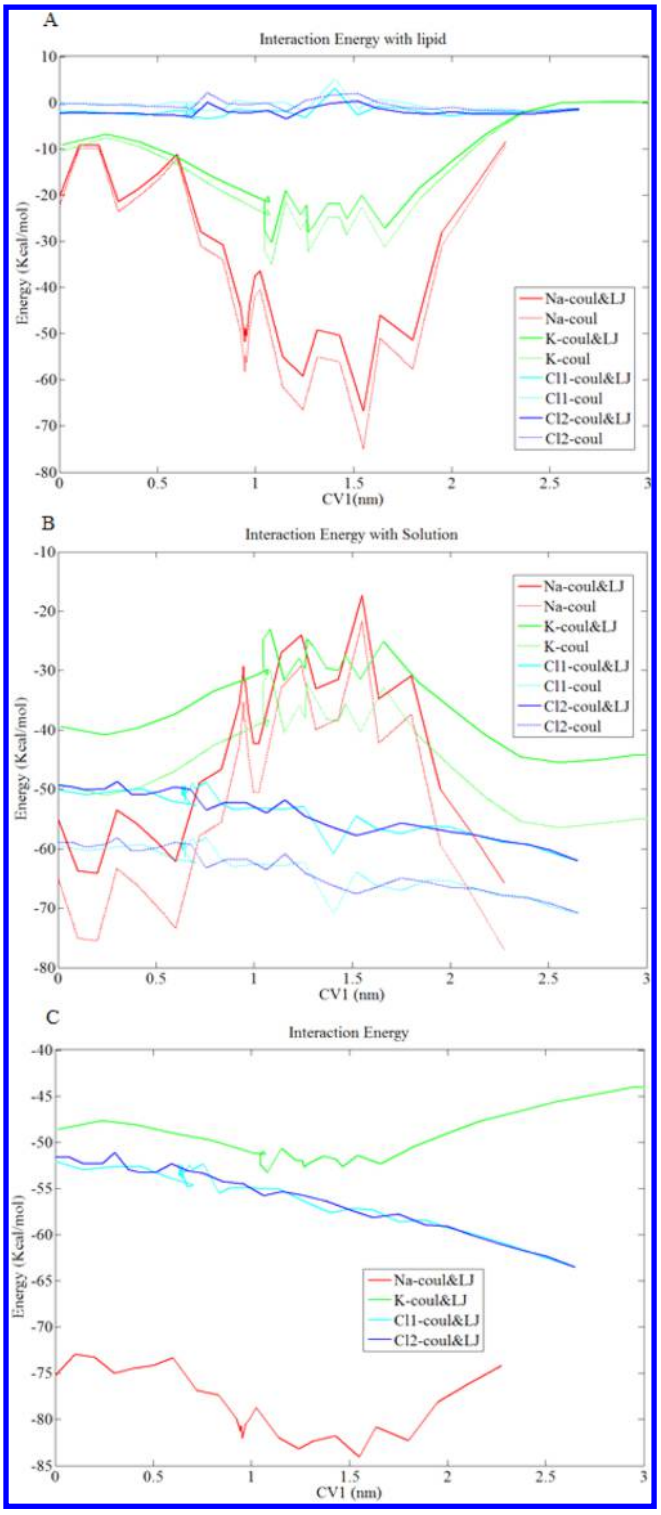


**Figure 7.** Interaction energy of ions with (A) lipids, (B) solution, and (C) system. In addition, the Coulomb force of ions with (A) lipids and (B) solution is also drawn in thinner lines.

stronger water wire is likely to strengthen the interactions between water and the ion.

Interaction energy between the ion and the whole system, namely the sum of the interaction energies between the ion and lipid, and between the ion and water solution, is shown in Figure 7C. The general trend of $Na^+$ and $K^+$ is consistent, which is shown with achieving the minimum at the membrane hydrophilic region with large fluctuations which are apparently derived from the competition of lipid interaction energy and solution interaction energy with the ion, and the interaction energy is quite unfavorable when the ion is in the hydrophobic core. It is worth noting that the interaction energy of $Na^+$ is generally 25−30 kcal/mol lower than $K^+$, which is probably related with the stronger lipid interactions and larger water molecule amounts, considering the analysis and comparison on the lipid interaction energy and water solution interaction energy above. This may suggest the interaction energy between the ion and system largely depends on the degree of membrane deformation and the situation of water wires.

In contrast with the strong interactions between lipid headgroups and $Na^+$ or $K^+$, there are hardly any interactions between lipids and $Cl^-$; the interaction energy of $Cl^-$ with lipids are almost 0 kcal/mol during the whole process (Figure 7A). On the other hand, $Cl^-$ has strong interactions with water solution. After $Cl^-$ permeate into the membrane, CV1 < 2 nm, $Cl^-$ interaction energies with water solution increased slowly, probably caused by the loss of surrounding water molecules. However, even in the hydrophobic core of membrane, where $Cl^-$ brings less water molecules than $K^+$ (Figure 3), the interaction energy of $Cl^-$ with water is still lower than $K^+$. Since $Cl^-$ has stronger interactions with water molecules than $K^+$ even in bulk, and also $K^+$ interacts with not only water but also lipid headgroups around, the lower interaction energy of $Cl^-$ than $K^+$ in the hydrophobic core seems reasonable. Nevertheless, throughout the whole process, when the ion permeates from solution, CV1 = 2.3 nm, to the hydrophobic center, CV1 = 0 nm, the interaction energy of $K^+$ with solution only increases 2−3 kcal/mol, and $Na^+$ about 5 kcal/mol (with huge fluctuations), whereas interaction energy of $Cl^-$ increases about 8 kcal/mol, which suggests the more water molecules brought into the membrane by the cations has decreased the changes of solution interaction energies. Similarly, $Cl^-$ interaction energy with the system is slightly lower than $K^+$, but the increase in it from CV1 = 2.3 nm to CV1 = 0 nm is 8−9 kcal/mol, and the increase of $K^+$ is about 2−3 kcal/mol, of $Na^+$ is almost 0 kcal/mol. In view of the changes of interaction energies with the system, the strong interactions with lipid headgroups and the more water molecules brought in help the cations, i.e. $Na^+$ and $K^+$, suffering less energetically uncomfortable in the hydrophobic core of membrane.

The interaction energies with lipids agree well with our analysis on lipid formations above. More importantly, concerning the waterwire mediated pathways, the stronger interaction energies with lipids an ion has, it will cause larger membrane deformation, and also thicker and shorter water wire, and further the free energy barrier of it appeared to be lower. The comparisons of the three ions, $Na^+$, $K^+$, and $Cl^-$, show that, by affecting the interactions with lipids, the electrical properties of ions exert great influence on ions' permeations. It should be emphasized that the POPC lipids we used are comparatively thicker membranes.[47] Earlier research has suggested water wires may be not necessary in thin membranes,[48,49] in which a complete water pore may be formed by the touching of bilayers on both sides. On the other hand, for very thick membranes, a water bridge may be too difficult to form, just like the nonwaterwire pathway of $Cl^-$.[50−52] In the situation of $Cl^-$, there may exist a delicate balance that on one side an unbroken water wire is likely to decrease the energy barrier of permeating through the hydrophobic core, but on the other side, hydrophobic thickness


DOI: 10.1021/acs.jctc.6b00695
J. Chem. Theory Comput. 2016, 12, 4959−4969

of POPC membrane may be a little too large to form such a long water wire. Li et al. have proved that the energy barrier will become higher when permeating through thicker membranes, and in thicker membranes (of at least 18 carbons), a solubility model will be energetically favored over an ion-induced defect model.[51] As a result, water wire is not stable during the permeation of $Cl^-$. On the contrary, the cations, $Na^+$ and $K^+$, can easily pull the lipid headgroups in and reduce hydrophobic thickness, thus to form a shorter and stronger water wire.

Compared to the first waterwire mediated pathway, the configuration changes of $Cl^-$ in the second nonwaterwire pathway are quite simple, which may decrease the loss of entropies. The deuterium order parameters Scd of lipid tails in different pathways were calculated, as shown in Figure S2. The changes in the $Cl^-$ nonwaterwire pathway are a little smaller than the other three. In another point of view, the free energy barrier can be divided into three parts, the energy cost in membrane deformation, in forming the water bridge, and in moving the ion to the middle of the water bridge,[25] of which energy cost in forming the water bridge is the largest one.[25,53,54] Lack of a water bridge may help to largely decrease the free energy barriers in the nonwaterwire mechanism of $Cl^-$.

## 4. CONCLUSIONS

By employing an effective sampling method and collective variables, we found possible minimum free energy permeation pathways for monovalent ions, $Na^+$, $K^+$, and $Cl^-$, through thick POPC bilayers. $Na^+$ and $K^+$ are found to have similar water wire mediated permeation pathways, where ions permeate through a water wire connecting the hydrophobic−hydrophilic interfaces of both sides. $Cl^-$ has two possible pathways, one of which is also waterwire mediated, and the other one is not, in which the ion simply diffuses through with a solvated shell. The nonwaterwire pathway of $Cl^-$ is much more energetically favorable, which suggests $Cl^-$ may permeate through bilayers without a water bridge, similar to the solubility-diffusion model. Permeations of $Na^+$ and $K^+$ are likely to cause significant membrane deformations, while permeations of $Cl^-$ are not. It is worth mentioning that all the ions are necessarily hydrated even in the hydrophobic core of membrane. The free energy barriers from our simulations are in semiquantitative agreement with experiments. Comparisons and analyses on the distribution of oxygens and interaction energies showed that, concerning the waterwire mediated pathways, the stronger interaction energies with lipids an ion has, it will cause larger membrane deformation, and also thicker and shorter water wire, and further the free energy barrier of it appeared to be lower. Thus, electrical properties of ions may largely affect the permeation process by differently interacting with lipids and water solution.

## ■ ASSOCIATED CONTENT

### Supporting Information

The Supporting Information is available free of charge on the ACS Publications website at DOI: 10.1021/acs.jctc.6b00695.

Figures S1 and S2 (PDF)

## ■ AUTHOR INFORMATION


### Corresponding Authors

*E-mail: xuqin523@sjtu.edu.cn.

*E-mail: dqwei@sjtu.edu.cn.


### Notes

The authors declare no competing financial interest.

## ■ ACKNOWLEDGMENTS

Dong-Qing Wei is supported by grants from the National High-Tech R&D Program (863 Program Contract No. 2012AA020307), the National Basic Research Program of China (973 Program) (Contract No. 2012CB721000), and Ph.D. Programs Foundation of Ministry of Education of China (Contract No., 20120073110057). Qin Xu is supported by grants from National Natural Science Foundation of China for Young Scholars (Grant No. 31400704). Dong-Qing Wei and Qin Xu are supported by funding 2016YFA0501703 from the Ministry of Science and Technology of China.

## ■ REFERENCES


(1) Papahadjopoulos, D.; Miller, N. Phospholipid model membranes. I. Structural characteristics of hydrated liquid crystals. *Biochim. Biophys. Acta, Biomembr.* **1967**, *135* (4), 624−38.

(2) Johnson, S. M.; Bangham, A. D. Potassium permeability of single compartment liposomes with and without valinomycin. *Biochim. Biophys. Acta, Biomembr.* **1969**, *193* (1), 82−91.

(3) Hauser, H.; Phillips, M. C.; Stubbs, M. Ion permeability of phospholipid bilayers. *Nature* **1972**, *239* (5371), 342−4.

(4) Bangham, A. D.; Standish, M. M.; Watkins, J. C. Diffusion of univalent ions across the lamellae of swollen phospholipids. *J. Mol. Biol.* **1965**, *13* (1), 238−52.

(5) Hauser, H.; Oldani, D.; Phillips, M. C. Mechanism of ion escape from phosphatidylcholine and phosphatidylserine single bilayer vesicles. *Biochemistry* **1973**, *12* (22), 4507−4517.

(6) Paula, S.; Deamer, D. W. Membrane Permeability Barriers to Ionic and Polar Solutes. In *Curr. Top. Membr.*; Deamer, D. W., Kleinzeller, A., Douglas, M. F., Eds.; Academic Press: San Diego, 1999; Vol. Vol. *48*, pp 77−95.

(7) Parisio, G.; Stocchero, M.; Ferrarini, A. Passive membrane permeability: Beyond the standard solubility-diffusion model. *J. Chem. Theory Comput.* **2013**, *9* (12), 5236−5246.

(8) Marrink, S.-J.; Berendsen, H. J. Simulation of water transport through a lipid membrane. *J. Phys. Chem.* **1994**, *98* (15), 4155−4168.

(9) Tepper, H. L.; Voth, G. A. Mechanisms of Passive Ion Permeation through Lipid Bilayers: Insights from Simulations. *J. Phys. Chem. B* **2006**, *110* (42), 21327−21337.

(10) Paula, S.; Volkov, A. G.; Deamer, D. W. Permeation of Halide Anions through Phospholipid Bilayers Occurs by the Solubility-Diffusion Mechanism. *Biophys. J.* **1998**, *74* (1), 319−327.

(11) Paula, S.; Volkov, A. G.; Van Hoek, A. N.; Haines, T. H.; Deamer, D. W. Permeation of protons, potassium ions, and small polar molecules through phospholipid bilayers as a function of membrane thickness. *Biophys. J.* **1996**, *70* (1), 339−348.

(12) Vorobyov, I.; Olson, T. E.; Kim, J. H.; Koeppe, R. E., II; Andersen, O. S.; Allen, T. W. Ion-Induced Defect Permeation of Lipid Membranes. *Biophys. J.* **2014**, *106* (3), 586−597.

(13) Benjamin, L. Mechanism and dynamics of ion transfer across a liquid-liquid interface. *Science* **1993**, *261* (5128), 1558−1560.

(14) Luo, G.; Malkova, S.; Yoon, J.; Schultz, D. G.; Lin, B.; Meron, M.; Benjamin, I.; Vanýsek, P.; Schlossman, M. L. Ion Distributions near a Liquid-Liquid Interface. *Science* **2006**, *311* (5758), 216−218.

(15) MacCallum, J. L.; Bennett, W. F. D.; Tieleman, D. P. Distribution of Amino Acids in a Lipid Bilayer from Computer Simulations. *Biophys. J.* **2008**, *94* (9), 3393−3404.

(16) Tepper, H. L.; Voth, G. A. Protons May Leak through Pure Lipid Bilayers via a Concerted Mechanism. *Biophys. J.* **2005**, *88* (5), 3095−3108.

(17) Wilson, M. A.; Pohorille, A. Mechanism of Unassisted Ion Transport across Membrane Bilayers. *J. Am. Chem. Soc.* **1996**, *118* (28), 6580−6587.

(18) Leontiadou, H.; Mark, A. E.; Marrink, S. J. Ion transport across transmembrane pores. *Biophys. J.* **2007**, *92* (12), 4209−15.




DOI: 10.1021/acs.jctc.6b00695
J. Chem. Theory Comput. 2016, 12, 4959−4969

(19) Parsegian, A. Energy of an Ion crossing a Low Dielectric Membrane: Solutions to Four Relevant Electrostatic Problems. *Nature* **1969**, *221* (5183), 844−846.
(20) Allen, T. W. Modeling Charged Protein Side Chains in Lipid Membranes. *J. Gen. Physiol.* **2007**, *130* (2), 237−240.
(21) Li, L.; Vorobyov, I.; Allen, T. W. Potential of mean force and pKa profile calculation for a lipid membrane-exposed arginine side chain. *J. Phys. Chem. B* **2008**, *112* (32), 9574−87.
(22) Vorobyov, I.; Li, L.; Allen, T. W. Assessing atomistic and coarse-grained force fields for protein-lipid interactions: the formidable challenge of an ionizable side chain in a membrane. *J. Phys. Chem. B* **2008**, *112* (32), 9588−602.
(23) Hu, Y.; Liu, X.; Sinha, S. K.; Patel, S. Translocation Thermodynamics of Linear and Cyclic Nonaarginine into Model DPPC Bilayer via Coarse-Grained Molecular Dynamics Simulation: Implications of Pore Formation and Nonadditivity. *J. Phys. Chem. B* **2014**, *118* (10), 2670−2682.
(24) Mirjalili, V.; Feig, M. Density-Biased Sampling: A Robust Computational Method for Studying Pore Formation in Membranes. *J. Chem. Theory Comput.* **2015**, *11* (1), 343−350.
(25) Wang, Y.; Hu, D.; Wei, D. Transmembrane Permeation Mechanism of Charged Methyl Guanidine. *J. Chem. Theory Comput.* **2014**, *10* (4), 1717−1726.
(26) Dorairaj, S.; Allen, T. W. On the thermodynamic stability of a charged arginine side chain in a transmembrane helix. *Proc. Natl. Acad. Sci. U. S. A.* **2007**, *104* (12), 4943−8.
(27) Hirose, H.; Takeuchi, T.; Osakada, H.; Pujals, S.; Katayama, S.; Nakase, I.; Kobayashi, S.; Haraguchi, T.; Futaki, S. Transient focal membrane deformation induced by arginine-rich peptides leads to their direct penetration into cells. *Mol. Ther.* **2012**, *20* (5), 984−993.
(28) Khavrutskii, I. V.; Gorfe, A. A.; Lu, B.; McCammon, J. A. Free Energy for the Permeation of Na+ and Cl− Ions and Their Ion-Pair through a Zwitterionic Dimyristoyl Phosphatidylcholine Lipid Bilayer by Umbrella Integration with Harmonic Fourier Beads. *J. Am. Chem. Soc.* **2009**, *131* (5), 1706−1716.
(29) Friedman, H. L.; Jolicoeur, C.; Krishnan, C. V. Ionic Interactions in water. *Ann. N. Y. Acad. Sci.* **1973**, *204* (1), 79−99.
(30) Jaynes, E. T. Gibbs vs Boltzmann Entropies. *Am. J. Phys.* **1965**, *33* (5), 391−398.
(31) Ulmschneider, J. P.; Ulmschneider, M. B. United Atom Lipid Parameters for Combination with the Optimized Potentials for Liquid Simulations All-Atom Force Field. *J. Chem. Theory Comput.* **2009**, *5* (7), 1803−1813.
(32) Darden, T.; York, D.; Pedersen, L. Particle mesh Ewald: An N log(N) method for Ewald sums in large systems. *J. Chem. Phys.* **1993**, *98* (12), 10089−10092.
(33) Essmann, U.; Perera, L.; Berkowitz, M. L.; Darden, T.; Lee, H.; Pedersen, L. G. A smooth particle mesh Ewald method. *J. Chem. Phys.* **1995**, *103* (19), 8577−8593.
(34) Kumar, S.; Bouzida, D.; Swendsen, R. H.; Kollman, P. A.; Rosenberg, J. M. The weighted histogram analysis method for free-energy calculations on biomolecules. I: The method. *J. Comput. Chem.* **1992**, *13* (8), 1011−1021.
(35) Grossfield, A. WHAM: the weighted histogram analysis method.
(36) Flewelling, R. F.; Hubbell, W. L. Hydrophobic ion interactions with membranes. Thermodynamic analysis of tetraphenylphosphonium binding to vesicles. *Biophys. J.* **1986**, *49* (2), 531−540.
(37) Franklin, J. C.; Cafiso, D. S. Internal electrostatic potentials in bilayers: measuring and controlling dipole potentials in lipid vesicles. *Biophys. J.* **1993**, *65* (1), 289−299.
(38) Vorobyov, I.; Bekker, B.; Allen, T. W. Electrostatics of Deformable Lipid Membranes. *Biophys. J.* **2010**, *98* (12), 2904−2913.
(39) Nichols, J. W.; Abercrombie, R. F. A view of hydrogen/hydroxide flux across lipid membranes. *J. Membr. Biol.* **2010**, *237* (1), 21−30.
(40) Mancinelli, R.; Botti, A.; Bruni, F.; Ricci, M. A.; Soper, A. K. Hydration of Sodium, Potassium, and Chloride Ions in Solution and the Concept of Structure Maker/Breaker. *J. Phys. Chem. B* **2007**, *111* (48), 13570−13577.
(41) Papahadjopoulos, D.; Nir, S.; Ohki, S. Permeability properties of phospholipid membranes: effect of cholesterol and temperature. *Biochim. Biophys. Acta, Biomembr.* **1972**, *266* (3), 561−583.
(42) Rao, B. G.; Singh, U. C. A free energy perturbation study of solvation in methanol and dimethyl sulfoxide. *J. Am. Chem. Soc.* **1990**, *112* (10), 3803−3811.
(43) Rao, B. G.; Singh, U. C. Hydrophobic hydration: a free energy perturbation study. *J. Am. Chem. Soc.* **1989**, *111* (9), 3125−3133.
(44) Åqvist, J. Ion-water interaction potentials derived from free energy perturbation simulations. *J. Phys. Chem.* **1990**, *94* (21), 8021−8024.
(45) Marcus, Y. Thermodynamic functions of transfer of single ions from water to nonaqueous and mixed solvents: Part I-Gibbs free energies of transfer to nonaqueous solvents. *Pure Appl. Chem.* **1983**, *55* (6), 977−1021.
(46) Dang, L. X.; Rice, J. E.; Caldwell, J.; Kollman, P. A. Ion solvation in polarizable water: molecular dynamics simulations. *J. Am. Chem. Soc.* **1991**, *113* (7), 2481−2486.
(47) Kučerka, N.; Nieh, M.-P.; Katsaras, J. Fluid phase lipid areas and bilayer thicknesses of commonly used phosphatidylcholines as a function of temperature. *Biochim. Biophys. Acta, Biomembr.* **2011**, *1808* (11), 2761−2771.
(48) E, W.; Ren, W.; Vanden-Eijnden, E. Minimum action method for the study of rare events. *Commun. Pure Appl. Math.* **2004**, *57* (5), 637−656.
(49) E, W.; Vanden-Eijnden, E. Towards a theory of transition paths. *J. Stat. Phys.* **2006**, *123* (3), 503−523.
(50) MacCallum, J. L.; Bennett, W. D.; Tieleman, D. P. Transfer of arginine into lipid bilayers is nonadditive. *Biophys. J.* **2011**, *101* (1), 110−117.
(51) Li, L. B.; Vorobyov, I.; Allen, T. W. The role of membrane thickness in charged protein−lipid interactions. *Biochim. Biophys. Acta, Biomembr.* **2012**, *1818* (2), 135−145.
(52) Li, L.; Vorobyov, I.; Allen, T. W. The different interactions of lysine and arginine side chains with lipid membranes. *J. Phys. Chem. B* **2013**, *117* (40), 11906−11920.
(53) Tieleman, D. P.; Marrink, S.-J. Lipids Out of Equilibrium: Energetics of Desorption and Pore Mediated Flip-Flop. *J. Am. Chem. Soc.* **2006**, *128* (38), 12462−12467.
(54) Wohlert, J.; den Otter, W. K.; Edholm, O.; Briels, W. J. Free energy of a trans-membrane pore calculated from atomistic molecular dynamics simulations. *J. Chem. Phys.* **2006**, *124* (15), 154905.


DOI: 10.1021/acs.jctc.6b00695
*J. Chem. Theory Comput.* 2016, 12, 4959−4969